J Mater Sci (2009) 44:3229–3234
DOI 10.1007/s10853-009-3432-9

Electrical, thermal, and dielectric properties of $PbZr_{1-x}Sn_xO_3$ ($0 \leq x \leq 0.3$) single crystals

I. Jankowska-Sumara · A. Majchrowski · J. Żmija

Received: 29 December 2008 / Accepted: 20 March 2009 / Published online: 7 April 2009

Abstract $PbZrO_3$ and mixed $PbZr_{1-x}Sn_xO_3$ single crystals were grown by means of high temperature solution growth technique. A spontaneous crystallization was carried out in a Pt crucible, with PbO as a solvent. Electrical as well as thermal and dielectric properties were investigated in terms of Sn concentration. The measurements have been made in the large temperature range between 120 K and 800 K. The temperature dependences of c_p for investigated crystals can be approximated by the Einstein function and at high temperatures (cubic phase) c_p reaches the classical Dulong–Petit limit value $\sim$125 J/mol K. From electrical measurements the ac and dc conductivity and the activation energies have been calculated and attributed to different types of electrical conductivity.

Introduction

Since the discovery of antiferroelectricity in the perovskite structure in the lead zirconate $PbZrO_3$, materials exhibiting antiferroelectric behaviors has been extensively studied both in the experimental and theoretical way [1–6]. From the point of view of applications, the antiferroelectric materials are commonly used as energy storage devices.

$PbZrO_3$ is an object of the intensive studies because of the nature and origin of its phase transitions. It undergoes a typical I-order phase transition at about 510 K from an antiferroelectric (orthorhombic) to paraelectric (cubic) phase [7, 8]. In literature there are reports of two kinds of $PbZrO_3$, with and without a transient ferroelectric phase appearing just below T_c [9]. The existence of this transient phase is closely related to the point defects in the Pb/O sublattices which are easily produced in the technological process. X-ray, Raman light scattering, and dielectric measurements [10] showed that crystals without the transient phase are structurally more perfect, than those with the transient phase. The range and stability of the transient phase can be modified by different substitutions at the Pb and/or Zr sites. Usually foreign ions stabilize the rhombohedral ferroelectric phase below T_c or induce polar regions in the paraelectric phase. This is important from the point of view of different industrial applications. A lot of researches have been done on solid solutions containing Ti like $PbZr_{1-x}Ti_xO_3$, or Ba like $Pb_{1-x}Ba_xZrO_3$ [11–16].

On the other hand it has been shown in our previous articles, that a small amount of Sn ions in $PbZrO_3$ cancels the possibility of the appearance of ferroelectric transient phase and strengthens the first order character of phase transition [17]. For higher concentrations of Sn the decrease in the transition temperature T_c can be observed and a new transient phase below T_c which was established to be also antiferroelectric one appears. For the Sn concentrations higher than $x = 0.3$, a third phase of the ferroelectric arrangement is induced. A detailed phase transitions sequence is presented in [18, 19].

The change of the character of phase transitions was also observed. While below $x = 0.2$ the first order of phase transitions is maintained, above $x = 0.2$ the gradual change to the second order is observed. A tricritical point was postulated to exist near the concentration $x = 0.3$ in $PbZr_{1-x}Sn_xO_3$.

I. Jankowska-Sumara (✉)
Institute of Physics, Pedagogical University, ul. Podchorążych 2, Kraków 30-084, Poland
e-mail: ijsumara@ap.krakow.pl

A. Majchrowski · J. Żmija
Institute of Applied Physics, Military University of Technology, ul. Kaliskiego 2, Warsaw 00-908, Poland

The aim of the present work is to study the effect of Sn substitution on antiferroelectric and ferroelectric properties of chemically homogeneous and stoichiometric $PbZr_{1-x}Sn_xO_3$ single crystals. The new crystals of $PbZr_{1-x}Sn_xO_3$ (abbreviated in the text as PZS-x) have been obtained and some of their physical properties have been tested. Detailed thermal, dielectric, and electrical conductivity measurements have been performed.

Crystal growth and experimental details

Pure lead zirconate $PbZrO_3$ and mixed $PbZr_{1-x}Sn_xO_3$ ($x \leq 0.3$) crystals were grown using a high temperature solution growth (flux) method due to the spontaneous crystallization. An one-zone resistance furnace controlled with the Eurotherm 2704 microprocessor regulator allowed to change the rate of heating/cooling of the melt in a very broad range, from 300 K/h to 0.1 K/h. As a solvent PbO–B_2O_3 mixture was used. The composition of the melt used in our experiments was the same as in Ref. [20]: 2.4 mol percent of $PbZrO_3$ or $PbZr_{1-x}Sn_xO_3$, 77 mol percent of PbO, and 20.6 mol percent of B_2O_3. The total mass of the melt was 140 g. The melt was synthesized directly in a Pt crucible, then covered with a Pt lid and heated up to 1350 K. The temperature gradient in the melt was kept around 5 K/cm. The temperature measured under the bottom of crucible, was kept for at least 3 h so as to enable complete soaking of the melt, and then it was lowered at the rate of 2 K/h down to 1120 K. In the following step the remaining melt was decanted and as-grown crystals attached to the crucible walls were cooled down to room temperature at a rate of 10 K/h. The dark gray crystals in the form of cubes and rectangular prisms were obtained.

The chemical composition of crystals has been verified from energy dispersive spectrometry (EDS) measurements using a scanning electron microscopy (SEM) with Hitachi S4700 apparatus. To perform measurements the crystals were cut into plates with average dimensions of $3 \times 2 \times 0.5$ mm^3. For dielectric and conductivity measurements the plates were covered with silver electrodes. The electrical properties were determined in the frequency range of 100 Hz–100 kHz with HP 4363 LCR meter and 6517A Keithley electrometer (in case of dc conductivity). A home made furnace was used to heat the samples from room temperature to 820 K.

The specific heat measurements were made using a Netzsch DSC F3 Maia calorimeter in the temperature range from 120 K to 820 K under the argon atmosphere at the flow rate 30 mL/min. The specimen consisted of single piece of crystal of the average mass 20 mg which was placed in an alumina crucible. The data were collected both on heating and cooling process.

Dielectric properties

The compositional dependence of dielectric response characteristics for $PbZr_{1-x}Sn_xO_3$ crystals is shown in Fig. 1 for x from 0 to 0.3. For pure $PbZrO_3$ the dielectric permittivity reaches the maximum at $T_c = 510$ K. The maximum of ε' is independent on frequency which is characteristic of a "classical ferro- or antiferroelectric," contrary to a "relaxor." There is only one maximum on $\varepsilon'(T)$ dependence both on heating and on cooling. No additional anomaly corresponding to the transient ferroelectric phase was detected. The lack of such kind of anomaly speaks for the high quality of crystals.

While $PbZrO_3$ undergoes one phase transition at T_c, in PZS with Sn content a transient antiferroelectric phase just below T_c appears. More information about phase transitions sequence in the investigated samples can be found in [17–19].

Thermal properties

The measurements of specific heat in the range of 120 K–820 K are presented in Fig. 2. The anomalies observed as peaks on the $c_p(T)$ dependences correspond to the temperatures of the first order phase transitions observed also in the dielectric measurements [17–19]. The peaks near the first order phase transition are usually large and narrowly centered. For the composition $x = 0.3$ a very small anomaly observed at T_c suggests that this anomaly is associated rather with the second order phase transition. Thus, the tricritical point, i.e., the composition at which the first order transition becomes the second order one is close to this composition ($x = 0.3$). The calculated values of latent heat and entropies associated with the phase transitions in the function of composition are presented in Table 1.

On the basis of statistical model, the entropy change for order–disorder phase transition is about 4 J/mol [21]. The lowering value of entropy thus indicates the change from order–disorder to displacive type of phase transition. As the concentration of x increases in PZS (above $x = 0.2$) the value of entropy corresponding to T_c slightly decreases. So the conclusion can be made that for the PZS crystals the phase transition to cubic phase is neither purely order–disorder, nor displacive type. The similar conclusion was made on the basis of Raman scattering and dielectric relaxations measurements for $PbZrO_3$ and PZT single crystals [22].

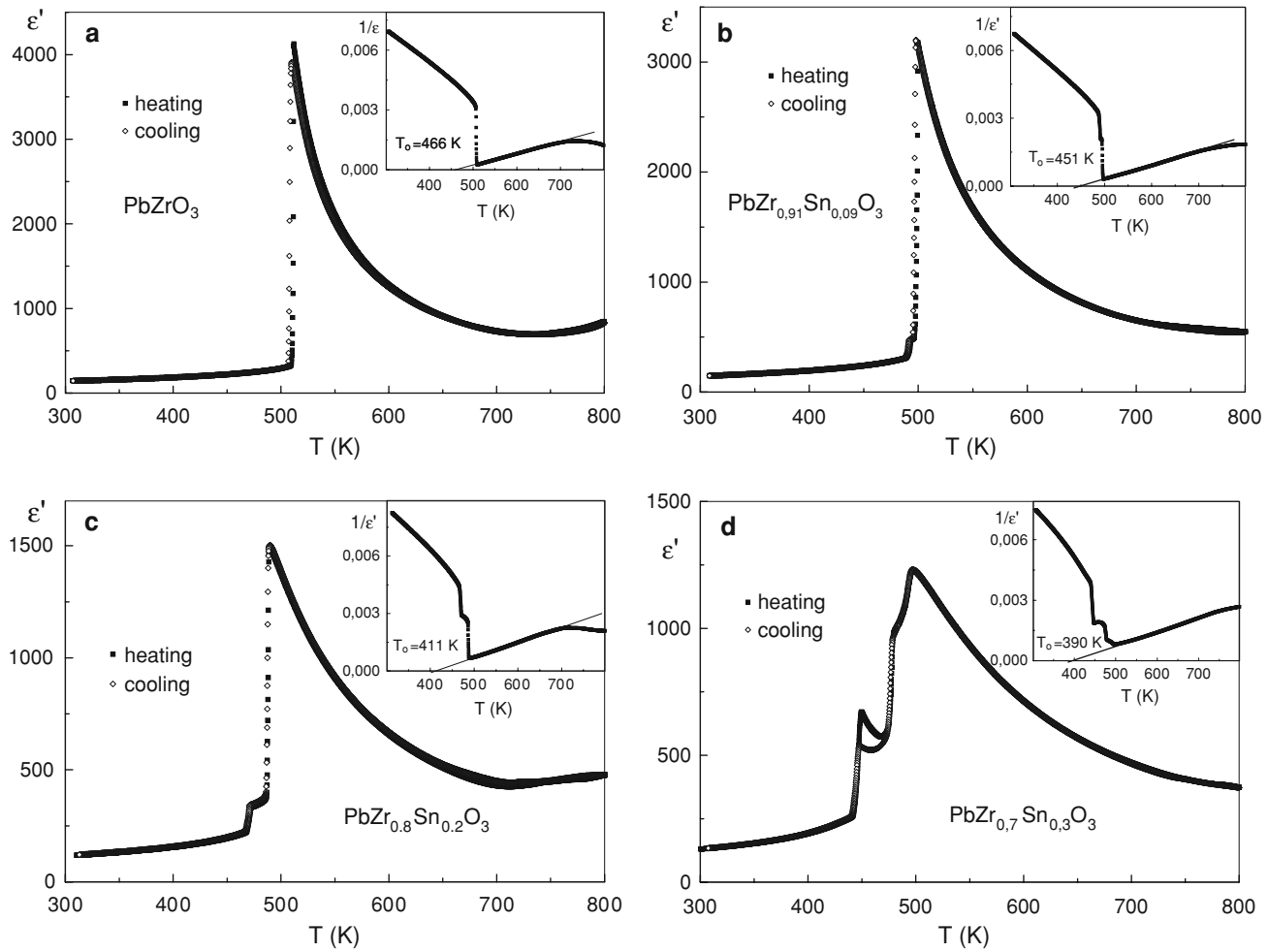

Fig. 1 Temperature dependences of the real part of ε' (T) for different compositions of PZS-x crystals measured at the frequency 100 kHz. The insets show the Curie–Weiss law obeyed in paraelectric phase

In the cubic phase above T_c the heat capacity reaches the values close to 125 J/mol K. This value is nearly identical to a classical Dulong–Petit limit $c_v \approx c_p = 3nK_BN_A =$ 124.7 J/mol K, where, n is the number of atoms per unit cell, K_B is the Boltzmann's constant, and N_A is the Avogadro number. The small deviations from this value are most probably associated with the small concentration of point defects.

It is possible to approximate the temperature dependence of c_v by the well-known Einstein's equation:

$$c_v = 3N_AK_B\left(\frac{\Theta_E}{T}\right)^2\frac{e^z}{(e^z-1)^2} \text{ where, } z=\frac{\Theta_E}{T}. \quad (1)$$

This expression describes better the $c_v(T)$ dependence at higher temperatures than the Debye function which fits better at very low frequencies. At high temperature limit the c_v tends to a constant value $3N_AK_B = 3R$ which is in agreement with the Doulong–Petit law.

At low temperatures the expression takes much simpler form, i.e.,

$$c_v \cong 3N_AK_B\left(\frac{\Theta_E}{T}\right)^2 e^{-\frac{\Theta_E}{T}}. \quad (2)$$

By fitting the above function to the experimental data one can obtain the characteristic temperature θ_E. The value of this temperature enables us to establish the kind of interactions between atoms in the investigated crystal. For crystals with covalent bonds the characteristic temperature is high. For ionic bonds this value lowers ($\sim$300 K) [23].

The values of θ_E calculated from fits are presented in Table 1 in function of composition. The characteristic temperature increases from 717 K for pure $PbZrO_3$ to 849 K for PZS-0.3. This increase suggests that in a PZS-x system the atomic interactions change from ionic–covalent to covalent one. This experimental fact is in good agreement with the covalency model of Thoman [24, 25]. According to this

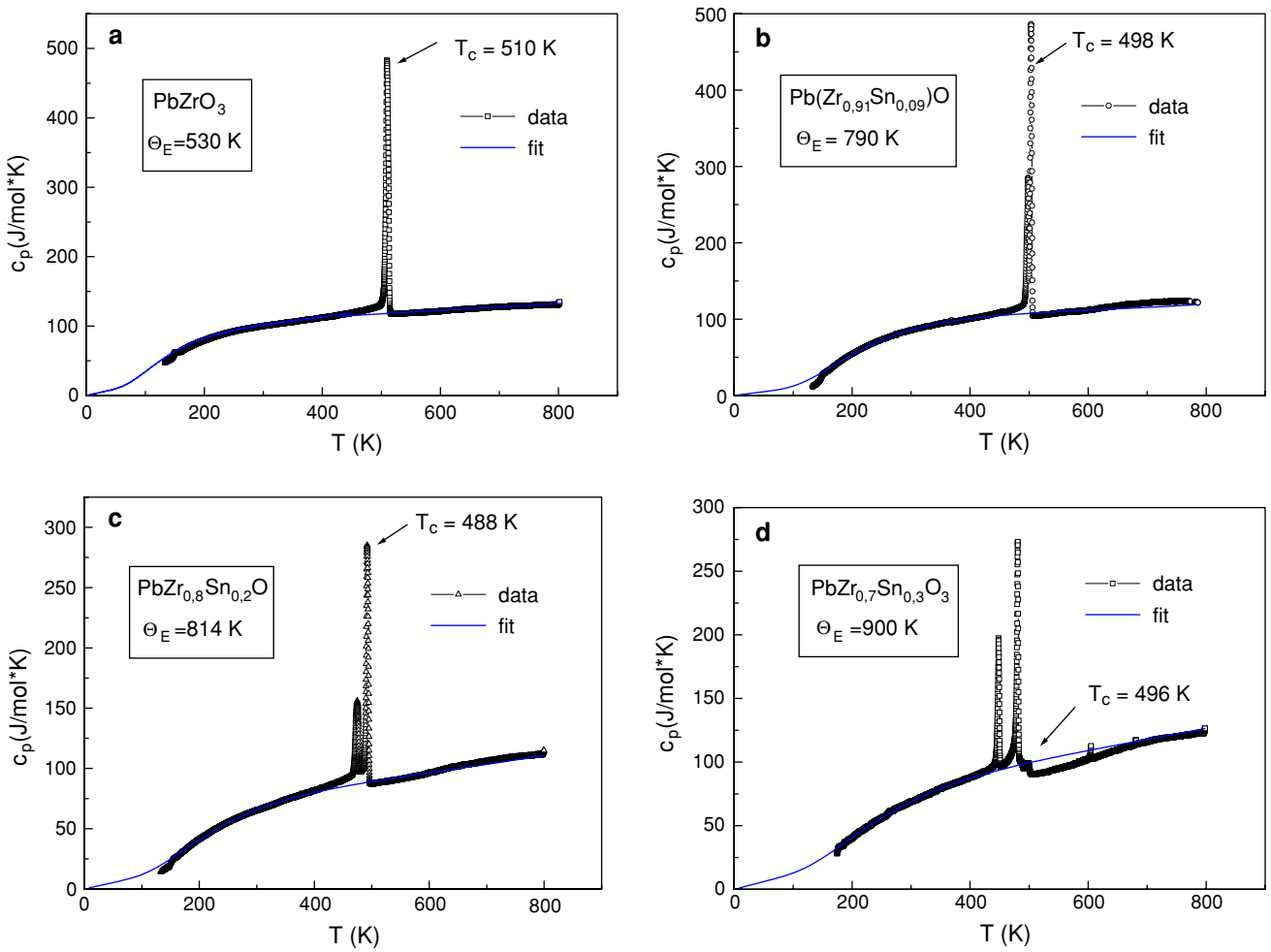

Fig. 2 Temperature dependences of the specific heat for different compositions of PZS-*x* crystals. *Solid lines* represent an approximation to the Einstein model

Table 1 The parameters of the phase transitions in PZS-*x* compounds taken from dielectric and specific heat measurements

Sample	T_c (K) from dielectric measurements	ε_{max} (at T_c)	T_c (K) from specific heat measurements	ΔE (J/mol) total latent heat	ΔS (J/mol · K) total entropy	Θ_E (K)
$PbZrO_3$	511	4200	510	2272	4.64	530
$PbZr_{0.91}Sn_{0.09}O_3$	499	3200	498	2405	4.75	790
$PbZr_{0.8}Sn_{0.2}O_3$	490	1520	488	1556	3.44	810
$PbZr_{0.7}Sn_{0.3}O_3$	497	1240	496	1693	3.55	900

model the decrease of average electronegativity leads to a transformation from ionic to covalent interactions and accounts for the ferroelectric lattice distortion. The electronegativity calculated for the PZS-*x* system changes from 1.9 for pure $PbZrO_3$ to 1.83 for PZS-0.4 [18].

Ac and dc conductivity

The ac conductivity is the real part of the complex conductivity σ^* and is linked to the ε^* by the formulae:

$$\sigma^* = \omega\varepsilon_o\varepsilon'' + i\omega\varepsilon_o\varepsilon'$$
$$\sigma_{ac} = \omega\varepsilon_o\varepsilon'' \quad (3)$$

where, ω is the angular frequency.

The ac conductivity was measured as a function of frequency and temperature in the range from room temperature to 800 K. The evolution of σ_{ac} and σ_{dc} is presented in Fig. 3a and b for two different compositions as the function of $1/T$. This presentation enables us to calculate activation energies E_a using the well-known Arrhenius formula $\sigma(T) = \sigma_o \exp(-E_a/K_B T)$. Generally two regions

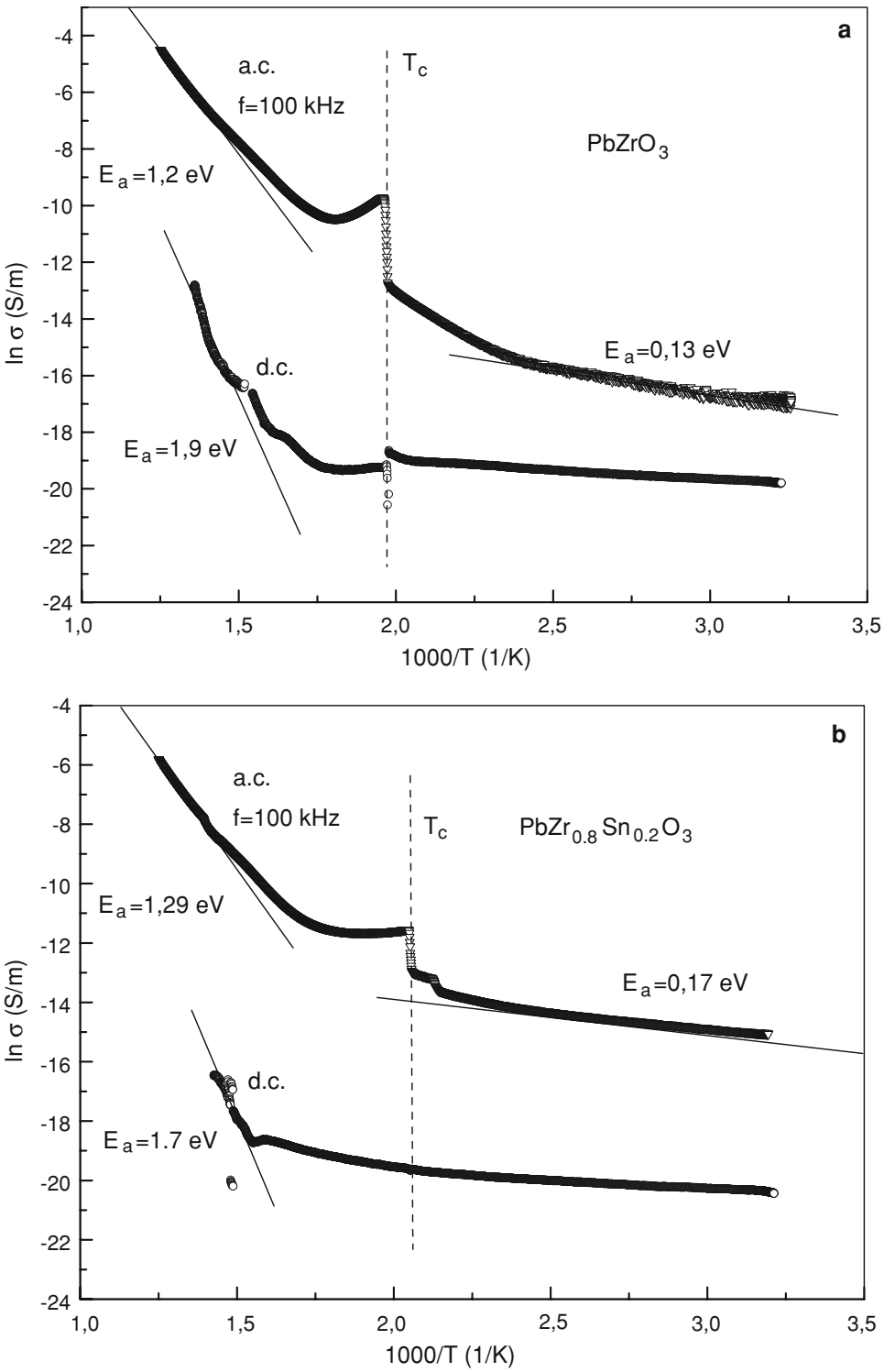

Fig. 3 Evolution of σ_{ac} and σ_{dc} as a function of inverse of temperature for PZS-x crystals: **a** $x = 0$ and **b** $x = 0.2$

with different activation energies can be distinguished. It is possible to link each region to the movement of electrical charges which are thermally activated.

At temperatures below T_c the activation energies are very low: 0.1–0.3 eV. They are attributed to electron jumps. The existence of conduction electrons is due to a deficiency in oxygen in $PbZrO_3$ as well as PZS-x. Above T_c the activation energies are of the range 1.2–1.4 eV and are attributed to bigger charges than those of electrons. It is due to oxygen vacancy movements [26, 27].

The large values of dc conductivity at high temperatures in the paraelectric phase are most probably attributed to free ionic charges stored at the two dielectric-electrode interfaces causing *space charge* [28].

Table 2 The values of the activation energies accompanying different types of electric conductivity

Sample	E_a (eV) low temperature ac conductivity	E_a (eV) high temperature ac conductivity	E_a (eV) high temperature dc conductivity
$PbZrO_3$	0.13	1.2	1.9
$PbZr_{0.91}Sn_{0.09}O_3$	0.13	1.13	1.43
$PbZr_{0.8}Sn_{0.2}O_3$	0.17	1.29	1.7
$PbZr_{0.7}Sn_{0.3}O_3$	0.31	1.4	2

The values of the activation energies accompanying three different types of conductivity are collected in Table 2.

Conclusions

$PbZr_{1-x}Sn_xO_3$ single crystals were grown and their dielectric, thermal, and electric properties were investigated. Each sample constituted single phase with perovskite structure.

The substitution of Sn^{4+} ions at the Zr^{4+} sites in PZS-x single crystals does not alter the basic structure of $PbZrO_3$ which crystallizes in an orthorhombic structure. The transition temperature T_c of these antiferroelectric compounds decreases with the increase of Sn concentration up to the $x = 0.25$. Near $x = 0.3$ T_c increases again and a ferroelectric transient phase is induced in these solid solutions [18, 19]. The phase transition at T_c is becoming more displacive and changes to a second order together with the increase of Sn above $x = 0.2$. The increase of Sn concentration leads also to a transformation from ionic to covalent interactions between atoms. This is evidenced in the increasing value of the characteristic temperature in the $c_p(T)$ dependence. The covalent interactions are finally responsible for a ferroelectric lattice distortion.

The study of ac and dc electrical conductivity at a wide temperature range showed different mechanisms of thermally activated charges:

- Free electrons at low temperatures which are due to the deficiency in oxygen atoms,
- Movement of oxygen vacancies activated at higher temperatures,
- Migration of oxygen ions towards the electrodes, creating a non-ferroelectric interface which generates a Maxwell–Wagner effect giving a contribution to the dc electric conductivity at high temperatures. The low concentration of Sn ions initially decreases the concentration of free ionic charges. The increasing amount of Sn (above $x = 0.2$) increases again the dc conductivity via increasing the concentration of defects. The conclusion can be made here that the small amount of Sn ions in $PbZrO_3$ single crystals makes the crystal lattice structurally more perfect and decreases the electric conductivity.

Acknowledgement This work was partially supported by the State Committee of Scientific research (KBN).

References

1. Sawaguchi E (1953) J Phys Soc Jpn 8:615
2. Hańderek J, Ujma Z (1977) Acta Phys Pol A 51:87
3. Whatmore RW, Clarke R, Glazer AM (1978) J Phys C: Solid State Phys 11:3089
4. Roleder K (1980) Acta Phys Pol A 58:623
5. Roleder K (1988) Ferroelectrics 81:1217
6. Jankowska I, Roleder K, Dec J (1993) Ferroelectrics 150:436
7. Fujishita H, Shiosaki Y, Achiva A, Sawaguchi E (1982) J Phys Soc Jpn 51:3583
8. Corker DL, Glazer AM, Dec J, Roleder K, Whatmore R (1997) Acta Crystallogr B53:135
9. Roleder K, Dec J (1983) J Phys Condens Matter 1:1503
10. Dec J, Kwapuliński J (1989) Phase Transitions 18:1
11. Jaffe B, Cook W, Jaffe H (1971) Piezoelectric ceramics. Academic Press, New York
12. Viehland D (1995) Phys Rev B 52:778
13. Noheda B, Gonzalo JA, Cross LE, Guo R, Park SE, Cox DE, Shirane G (2000) Phys Rev B 61:8687
14. Roberts S (1951) Phys Rev B 81:1078
15. Shirane G (1952) Phys Rev B 86:219
16. Pakharel BP, Pandy D (2000) J Appl Phys 88:5364
17. Jankowska-Sumara I, Dec J, Miga S (2003) Mater Sci Eng B 103:94
18. Jankowska-Sumara I, Dec J (2004) Ferroelectrics 313:81
19. Jankowska-Sumara I (2007) Phys Stat Solidi b 244:1887
20. Dec J, Roleder K, Stróż K (1996) Solid State Commun 99:157
21. Smoleński GA, Krajnik NN (1968) Segnietoelektriki i Antisegnietoelektriki, Izd. Nauka, Moscow
22. Roleder K, Jankowska-Sumara I, Kugel GE, Maglione M, Fontana MD, Dec J (2000) Phase Transitions 71:287
23. Janik JM (1989) Fizyka Chemiczna (Chemical physics). PWN, Warszawa
24. Thoman H (1984) Siemens Forsch-u Entwickl-Ber Bd 13:1
25. Thoman H (1987) Ferroelectrics 73:183
26. Fasquelle D, Carru JC (2008) J Eur Ceram Soc 28:2071
27. Barranco AP, Pinar FC, Martinez OP, De Los Santos Guerra J, Carmenate IG (1999) J Eur Ceram Soc 19:2677
28. Jankowska-Sumara I, Roleder K, Dec J, Miga S (1995) J Phys Condens Matter 7:6137